



# An open-access WebApp for Inverse Laplace Transform analysis of TD-NMR signals

Tiago B. Moraes<sup>1</sup>, Gustavo V. Von Atzingen<sup>2</sup>, Larissa P. Mazzero<sup>1,2</sup>, William S. Mendes<sup>1,2</sup>, Marina B. Zacharias<sup>1</sup>, and Marcelo C. B. Cardinali<sup>1,2</sup>

<sup>1</sup>Universidade de São Paulo/ESALQ – Depto. Engenharia de Biossistemas – Av. Páduas Dias, 11 – 13418-900 – Piracicaba, SP – Brasil

<sup>2</sup>Instituto Federal de Educação, Ciência e Tecnologia de São Paulo – Câmpus Piracicaba – Rua Diácono Jair de Oliveira, 1005 – 13414-155, Piracicaba, SP – Brazil

**Correspondence:** Tiago B. Moraes (tiago.moraes@usp.br)

**Abstract.** Over recent years, compact and low-field time-domain nuclear magnetic resonance (TD-NMR) instruments have become increasingly available, expanding their use in the characterization of biomaterials across food, plant, and agro-industrial research. In this context, the Inverse Laplace Transform (ILT) has emerged as a powerful mathematical approach for extracting relaxation time distributions from TD-NMR signals. However, despite its widespread use, ILT analysis is often restricted to 5 proprietary software or requires advanced expertise in numerical methods, limiting its accessibility to non-specialist users. In this work, we present an open-access WebApp for performing ILT analysis of TD-NMR signals in a transparent and user-friendly manner. The implemented algorithm is based on non-negative least squares combined with Tikhonov regularization and singular value decomposition, allowing robust inversion of ill-posed relaxation data. The platform supports the main TD-NMR experiments used in practice, including Carr–Purcell–Meiboom–Gill (CPMG), Inversion Recovery, and Saturation Recovery 10 pulse sequences, and is compatible with data from instruments of any manufacturer. In addition to describing the mathematical formulation and implementation of the algorithm, a concise methodological discussion of ILT in the context of TD-NMR is provided. The performance of the WebApp is evaluated using both simulated datasets and representative experimental signals, demonstrating that the obtained relaxation time distributions are consistent with those produced by established ILT approaches. By lowering the barrier to advanced signal processing, the proposed WebApp represents a useful open scientific tool for 15 research and teaching in magnetic resonance applications.

## 1 Introduction

The two best-known Nuclear Magnetic Resonance (NMR) techniques in academia and industry are *Magnetic Resonance Imaging* (MRI) and *High-resolution NMR* (HR-NMR). The former is widely applied in radiology for non-invasive medical diagnostics, whereas the latter is a well-established analytical technique used in chemical analysis laboratories for the precise 20 characterization of molecular structures, playing a fundamental role in the pharmaceutical industry (Jacobsen, 2007; Blümich et al., 2014).



Time-domain NMR (TD-NMR), also referred to as *Low-field NMR* (LF-NMR) or *Low-resolution NMR* (LR-NMR) (Mitchell et al., 2014; Zalesskiy et al., 2014), is based on the same physical principles as MRI and HR-NMR, but employs simpler instrumentation based on permanent magnets, without the need for large superconducting systems or cryogenic liquids. As a result, 25 TD-NMR sensors and spectrometers have reduced size and cost, enabling the development of portable and benchtop instruments. These characteristics make TD-NMR a versatile technique for industrial and applied research, where it has increasingly been employed as a powerful analytical sensor. Recent advances in electronics and permanent magnet technology have further contributed to the reduction of production and maintenance costs, fostering the emergence of several companies dedicated to compact TD-NMR instrumentation, such as Bruker, Magritek, Oxford, Nanalysis, SpinLock, FIT, and Niumag (Bruker, 2023; 30 Magritek, 2023; Oxford, 2023; Nanalysis, 2023; SpinLock, 2023; FIT, 2023; Niumag, 2023).

For materials of biological origin, such as plants, foods, oils, seeds, and other agro-industrial products, magnetic resonance offers a non-destructive and nucleus-selective analytical approach, enabling the development of highly specific sensing methods. Among the available nuclei,  $^1\text{H}$  detection is the most commonly employed due to its high sensitivity, although the use of other nuclei has steadily increased in low-field NMR applications as instrumentation continues to improve (Blümich, 2016).

35 A wide variety of NMR methods can be implemented by applying different radio-frequency (rf) pulse sequences, resulting in distinct signal responses that encode diverse physicochemical information (Williams, 2005). The analysis of these signals is typically performed using mathematical approaches available in spectrometer software, including the *Fourier Transform* (FT), *exponential fitting*, the *Inverse Laplace Transform* (ILT), and, more recently, machine learning techniques (Engelsen and van den Berg, 2017). Despite these developments, advanced signal-processing algorithms—particularly ILT—are often 40 restricted to proprietary software or require specialized expertise, motivating many users to seek alternative implementations in environments such as C++, Python, MATLAB, or OriginLab (Moraes, 2021).

The objective of this paper is to present an open-access WebApp (<https://nmr-ilt.esalq.usp.br/>) for the application of the Inverse Laplace Transform (ILT) to time-domain NMR (TD-NMR) signals, together with a concise methodological discussion of the underlying principles. The implemented algorithm is based on a non-negative least squares approach combined with 45 Tikhonov regularization and singular value decomposition (SVD), enabling robust inversion of ill-posed relaxation data. In contrast to our previous ILT implementation reported in the literature Moraes (2021), which focused on local computational routines and specific applications, the present work provides a platform-independent, freely accessible Web-based framework suitable for TD-NMR data from instruments of any manufacturer. The platform supports the main TD-NMR experiments used in practice, including Carr–Purcell–Meiboom–Gill (CPMG), Inversion Recovery, and Saturation Recovery pulse sequences. 50 The main features of the proposed approach are validated using simulated datasets and representative experimental signals, demonstrating its consistency with established ILT methodologies and its potential as an open scientific tool for research and teaching in magnetic resonance applications.



## 2 Magnetic Resonance Background and Motivation for ILT

Magnetic resonance techniques can be broadly distinguished by magnetic field strength and homogeneity, which directly determine signal characteristics and the appropriate data analysis strategy. High-field NMR systems employ highly homogeneous magnetic fields, enabling frequency-domain analysis with high spectral resolution through the Fourier Transform (FT). In contrast, time-domain and low-field NMR (TD-NMR/LF-NMR) systems are typically based on permanent magnets, resulting in compact, cost-effective, and robust instrumentation, but often with limited magnetic field homogeneity.

In many TD-NMR and benchtop systems, magnetic field inhomogeneities prevent reliable frequency-domain resolution, making relaxometry-based approaches more suitable. Pulse sequences such as Carr–Purcell–Meiboom–Gill (CPMG), Inversion Recovery (IR), and related methods are therefore widely used to probe longitudinal ( $T_1$ ) and transverse ( $T_2$ ) relaxation processes. The signals acquired using these sequences consist of superpositions of exponentially decaying components, whose amplitudes and characteristic times reflect molecular dynamics and local interactions within the sample.

From a signal-processing perspective, relaxometry data represent an inverse problem in which the measured signal is modeled as a weighted sum of exponential decays. Unlike the Fourier Transform, which provides a direct and well-posed transformation, the determination of relaxation time distributions from TD-NMR signals constitutes an ill-posed inverse problem. In such cases, small perturbations in the input data—such as noise or experimental uncertainty—can lead to large variations in the recovered solution, necessitating the use of constrained optimization and regularization strategies.

Within this context, the Inverse Laplace Transform (ILT) has emerged as a powerful framework for analyzing TD-NMR relaxometry data. Practical implementations of the ILT rely on numerical algorithms that balance stability, resolution, and robustness through appropriate regularization and non-negativity constraints. These methodological aspects are central to the present work and motivate the development of a transparent, accessible, and reproducible platform for ILT-based analysis of TD-NMR signals, as described in the following section.

## 3 Inverse Laplace Transform

In time-domain and low-field NMR experiments, signal analysis is predominantly performed in the time domain, particularly through relaxometry-based methods. In heterogeneous systems, the measured signal generally reflects a superposition of contributions arising from distinct spin populations characterized by different relaxation times, leading to multiexponential signal behavior.

The present work does not aim to review relaxometry techniques in detail, which are extensively discussed elsewhere (Mitchell et al., 2014; Zalesskiy et al., 2014; Maus et al., 2006), but instead focuses on the mathematical processing of multiexponential signals acquired using pulse sequences such as Carr–Purcell–Meiboom–Gill (CPMG), Inversion Recovery (IR), Saturation Recovery (SR), and related methods.

In simple systems, relaxation data can often be adequately described by mono-exponential models. However, in more complex samples, the measured signal is better represented as a superposition of multiple exponential components, each associated



85 with a distinct relaxation time. In such cases, conventional multi-exponential fitting becomes unstable and strongly dependent on the assumed number of components.

In these situations, the analysis of relaxation data is commonly formulated as an inverse problem and addressed using Inverse Laplace Transform (ILT) methodologies, which aim to recover continuous distributions of relaxation times from experimental signals (Mitchell et al., 2014; Jacobsen, 2007; Moraes, 2021).

90 Figure 1 schematically illustrates the objective of ILT processing, in which a time-domain relaxometry signal is transformed into a relaxation time distribution. The positions and areas of the resulting peaks reflect the relative contributions of different spin populations present in the sample.

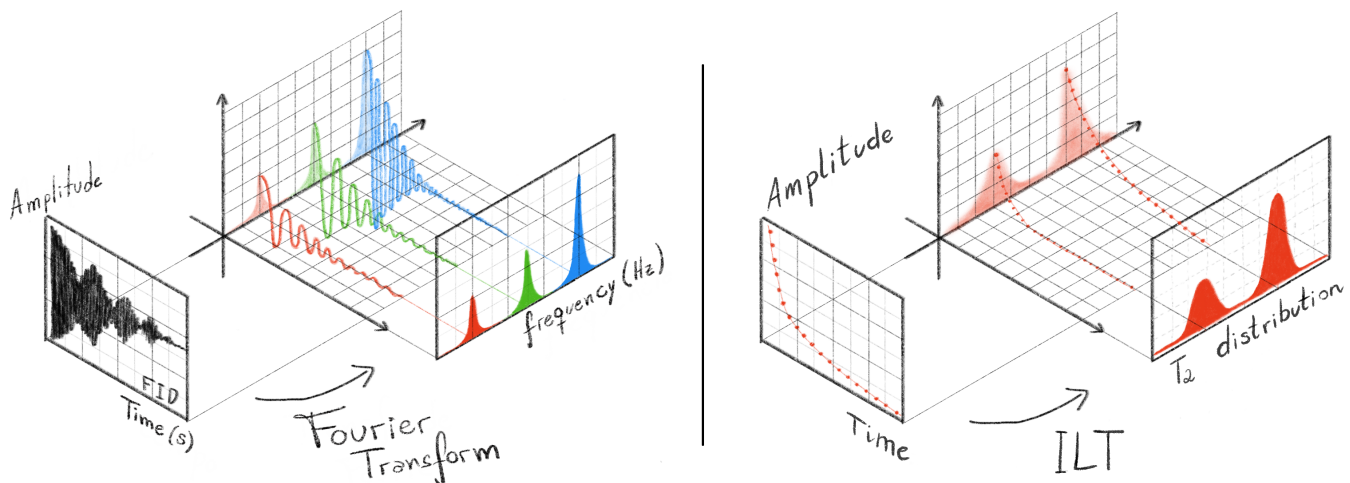


**Figure 1.** Comparative schematic illustration of time-domain NMR signal processing using the Fourier Transform (FT) and the Inverse Laplace Transform (ILT). In the FT approach (left panel), which is the most widely known and routinely used method in NMR spectroscopy, the Free Induction Decay (FID) consists of a mixture of oscillatory, exponentially damped sinusoids in the time domain. After Fourier transformation, these components are separated in the frequency domain, producing a spectrum whose peak positions, linewidths, and amplitudes provide chemical and structural information about the sample. In contrast, the ILT approach (right panel) is applied to non-oscillatory signals. On the left side of this panel, a Carr-Purcell-Meiboom-Gill (CPMG) type signal is represented by the echo amplitudes as a function of time, showing purely monotonic exponential decays rather than oscillations. By processing this signal with the ILT, the result is not a frequency spectrum but a distribution of relaxation times ( $T_2$ ), shown on the right, also called a relaxogram. The positions and areas of the  $T_2$  peaks reflect physical and compositional properties of the analyzed material, such as pore size distribution, water/oil content, and meat/fat ratio, among others. Together, the figure highlights the conceptual analogy between both transforms—each mapping time-domain signals into characteristic distributions—while emphasizing the fundamental difference between oscillatory (FT) and non-oscillatory (ILT) data.

In this way, the ILT process reveals the contribution of different spin groups, where the two wide peaks illustrated in the  $T_2$  distribution can be a better representation of a real sample, once real samples are not strictly homogeneous with singular



95 values of amplitude and relaxation times (narrow peaks), but they are actually inhomogeneous samples, with a dispersion of relaxation times.

The distribution obtained in the processing with the ILT can arise from an growing or decaying exponential damped curve, as CPMG ( $T_2$ ), or Inversion Recovery ( $T_1$ ), Saturation Recovery ( $T_1$ ), Diffusion (D), among other experiments, where what changes in the processing is the kernel equation used in the transformation, as will be discussed in the next section.

100 There are several software to perform this processing, some with free access and others being only supplied with licenses by the spectrometer manufacturing companies, each with different processing characteristics. The most famous ILT algorithms are CONTIN (*CONTINuous distribution*) (Provencher, 1982), OpenWin (*Uniform PENalty*) (Borgia et al., 1998), BRD (*Butler-Reeds-Dawson*) (Butler et al., 1981), TSVD (*Truncated Singular Value Decomposition*) (Fordham et al., 2017), NNLS (*non-negative least squares*) (Lawson and Hanson, 1976), PDCO (*Primal-Dual interior method*) (Berman et al., 2013), among 105 bi-dimensional ILT (Venkataraman et al., 2002; Bortolotti et al., 2019) and other methods.

110 In the next section, the basic concepts of the ILT and a simple-to-use WebApp developed for performing the transformation of TD-NMR signals are presented, freely available for research and teaching. A mathematical description of the implemented processing is then provided, followed by results with simulated and experimental data, and finally the procedures for using the program. A video tutorial demonstrating the code and its usage is available on the WebApp page or can be requested from the authors by email.

### 3.1 Mathematical description of the ILT

There are several mathematical approaches to perform the inversion of these TD-NMR signals, and these techniques are generally named as *Inverse Laplace Transform* by the NMR scientific community. It is worth noting that the method discussed here is different from the procedure of the same name found in Mathematical Physics books (Arfken and Weber, 1995). 115 Although the confusion with the name, the origin of the uses of this term by the NMR community is related to an analogy with the procedure of the Inverse Fourier Transform. Further details of this history can be found in the work of Fordham and colleagues (Fordham et al., 2017).

120 In the context of TD-NMR most of the pulse sequences used, the acquired signals are exponential and/or gaussian growth or decay. The inversion problem to resolve here is from an input signal  $s(t)$ , like equation ??, determine all the amplitudes and relaxations times present in the data. Therefore, what we call ILT is a particular case of a more general problem of inverting Fredholm Integral Equations, which can be written in the form:

$$f(x) = \int_a^b \phi(t) K(x, t) dt \quad (1)$$

where  $K(x, t)$  is the kernel function of the system, and the function  $\phi(t)$  represents the function to be determined from the experimental data curve  $f(x)$ .

125 In the case of an experimental signal from a CPMG (Carr-Purcell-Meiboom-Gill) pulse sequence, the input signal,  $c(t)$ , is given by  $c(t) = c(0).exp(-t/T_2)$ , where  $c$  represents the experimental signal,  $t$  is the time variable of the acquired signal, and



$T_2$  is the relaxation time. For a sample composed of multiple relaxation times, we have:

$$c(t) = \sum_{i=1}^k c_k(0) \exp(-t/T_{2i}) \quad (2)$$

where  $k$  denotes the number of components present in the sample.

130 In real complex samples, it is not physically expected to have only a singular value of relaxation time, but a continuous distribution of relaxation times. Thus, we can express the NMR signal as given by the integral:

$$c(t) = \int g(T_2) \exp(-t/T_2) dT_2 \quad (3)$$

where  $\exp(-t/T_2)$  is the kernel function and  $g(T_2)$  represents the distribution of relaxation times  $T_2$ , providing the amplitudes of each infinitesimal component  $dT_2$ .

135 ILT algorithm will determine the distribution of amplitudes  $g(T_2)$  from the experimental data  $c(t)$ , however experimental NMR signals  $c(t)$  are a set of  $n$  data points acquired over the time interval  $t$ , with the presence of experimental noise ( $\epsilon_n$ ), thereby:

$$c(t_n) = \sum_{i=1}^N g(T_{2i}) K(t_n, T_{2i}) + \epsilon_n \quad (4)$$

140 where  $K$  is the kernel equation of this summation. Note that  $N$  is the total points of the  $T_2$  dimension, which need to be defined in a window of expected relaxation times, for example, from 0.001 to 10 seconds using  $N = 100$  or 200 points. For a CPMG experiment, the kernel should be defined as a composition of decreasing exponential, as shown in equation 2. The inversion of this problem can be obtained through the minimization of the mean square errors, given by

$$X^2 = \|c(t) - F(t)\|^2 \quad (5)$$

145 where  $F(t)$  is the function that best describes the experimental data  $c(t)$ . This minimization problem is not trivial, as it involves a mathematically ill-posed problem (Istratov and Vyvenko, 1999; Venkataraman et al., 2002; Tikhonov, 1963).

Several regularization methods can be used to obtain solutions for this Fredholm integral problem, each presenting different characteristics of stability and reliability. Physically, in our TD-NMR experiments, it is reasonable to expect that our solution  $g(T_2)$  is a continuous distribution of relaxation times without the existence of delta peaks, discontinuous points, or negative values of amplitude in the distribution (Fig. 1). These constraints can be introduced into the program's algorithm through a 150 term that smooths the distribution and enforces non-negativity, as proposed by the NNLS (*non-negative least squares*) method. This regularization of the solution enforces more stable and continuous distributions, and the regularization parameter ( $\alpha$ ) is responsible for the smoothing of this solution.

Different values of regularization parameter  $\alpha$  can yield optimal curve fits, resulting in distributions with certain variations. Determining which distribution best represents the physical system is not trivial and, therefore, involves some subjectivity, as 155 the fit strongly depends on the signal-to-noise ratio of the data. Various methods have been used and proposed to optimize the choice of the regularization parameter  $\alpha$ , as the L-curve method (Hansen, 1992; Day, 2011). In the present implementation,



no automatic optimization strategy for the regularization parameter  $\alpha$  is employed. Instead,  $\alpha$  is selected by the user based on prior knowledge of the system and the signal-to-noise characteristics of the data, an approach commonly adopted in practical ILT analyses. Future versions of the WebApp will incorporate automated strategies for  $\alpha$  selection.

160 Therefore, the algorithm of the WebApp uses the Tikhonov Regularization method with singular value decomposition while assuming the non-negativity of the response, also known as NNLS (non-negative least squares), widely used by the NMR community.

#### 4 ILT-NMR WebApp

165 An open-access WebApp was developed to enable Inverse Laplace Transform (ILT) analysis of TD-NMR data without the need for local software installation. The application is deployed using Docker and hosted on secure servers of the University of São Paulo (USP) within the InterNuvem infrastructure, ensuring stable and reliable access for the scientific community. The computational core of the WebApp was implemented in Python (Van Rossum and Drake Jr, 1995), making use of established numerical and visualization libraries, including NumPy (Harris et al., 2020) and Plotly. The implemented algorithm represents a platform-independent adaptation of our previously reported ILT routine developed for OriginLab software (Moraes, 2021).

170 The WebApp supports ILT processing of relaxation data acquired using Carr–Purcell–Meiboom–Gill (CPMG), Inversion Recovery (IR), and Saturation Recovery (SR) pulse sequences. For each experiment type, the corresponding kernel function  $K(t, T)$  is defined as:

$$\begin{aligned} \text{CPMG: } K(t, T) &= [\exp(-t/T)] \\ \text{IR: } K(t, T) &= [1 - 2 \exp(-t/T)] \\ \text{SR: } K(t, T) &= [1 - \exp(-t/T)] \end{aligned} \tag{6}$$

where  $t$  denotes the experimental time axis and  $T$  represents the relaxation time domain of the resulting ILT distribution.

175 Figure 2 summarizes the data-processing workflow implemented in the WebApp. Input signals are provided as text-based files containing the experimental time axis and one or more corresponding signal amplitudes. After specifying the experiment type and processing parameters, the ILT inversion is performed and the resulting relaxation time distributions are returned in graphical and numerical formats, allowing direct inspection and further analysis.

180 The WebApp interface was designed to provide flexible control over key processing parameters, including the definition of the relaxation time window, discretization of the  $T$  axis, baseline correction, signal normalization, and the choice of the regularization parameter  $\alpha$ . While the present implementation requires manual selection of  $\alpha$ , this approach allows the user to incorporate prior knowledge of the sample and signal-to-noise characteristics into the analysis. Automated strategies for  $\alpha$  optimization will be incorporated in future versions of the platform. To facilitate reproducibility and broader use, the WebApp accepts multiple signals sharing a common time axis, enabling batch processing and comparative analysis of TD-NMR experiments.

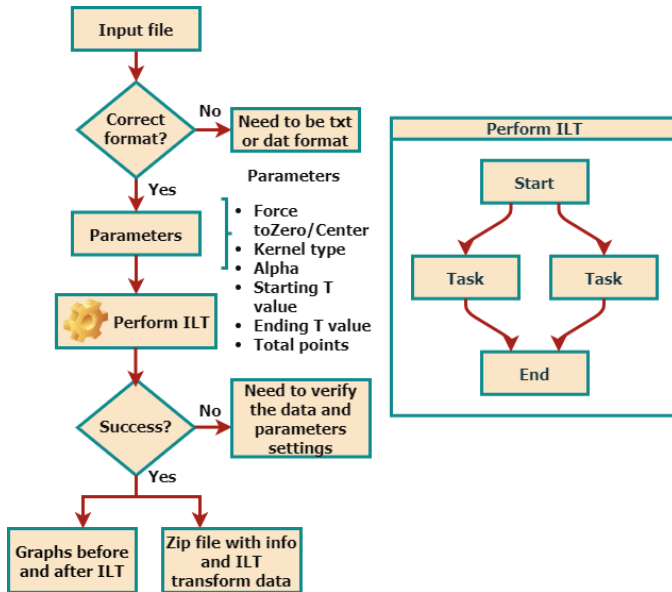


**Figure 2.** WebApp pipeline.

Figure 3 shows the Processing page of the User Interface, available at: <https://nmr-ilt.esalq.usp.br/>. The full navigation bar on the left includes Home (main page with general information about the ILT process), Processing (the core section for data processing), Citation, and Contact (to send a message to the authors).

At the Processing bar, it is required to inform the input parameters and information:

190 – **Kernel type:** Inform what type of data the User is processing. There are three options, CPMG, IR and SR kernels, equations 6;

195 – **Remove start points:** if desired, some initial points of the data can be removed. It is useful when delaying with spectrometer *dead-time* effects or spurious data points;

– **Alpha:** Regularization parameter  $\alpha$  is always necessary to be defined, and it is related to the *resolution* of the spectrum. Usually, the larger the  $\alpha$  value, the spectral resolution is lower, however forcing resolution can provide not reliable spectra in data with low signal-to-noise ratio. In this WebApp its value is defined by the User, typical values used are 0.01, 0.1, 1, 10.

– **Starting T value:** Set the minimum value of relaxation times expected, in the time scale defined ;

– **Ending T value:** Set the maximum value of relaxation times expected, in defined the time scale;

200 – **Number of points:** Total number of points in the resulting distribution spectrum. Typical values are 100 or 200;



**Figure 3.** WebApp simplified processing interface.

- **Time scale:** Inform if your time axis is in seconds, milliseconds or microseconds. After processing, the relaxation time T axis in the ILT spectra will be in the same order of magnitude;
- **Force to Zero/Center:** Spurious peaks can arise from a small displacement of the baseline input signals (*offset*), and this function can be used for this pre-processing of the input data;
- **Normalization:** this function will divided each column data by the first value of the signal, normalizing the signals;



- **Perform ILT:** Initiated the processing, in a few seconds (or minutes if many columns are inputted), the results are presented in Figures. Also an option to download all images and data points are available.

Note that the input data must be provided in a *.txt* or *.dat* file, where the first column represents the time axis and the second contains the signal intensity. Multiple signals can also be processed simultaneously by placing them in the subsequent columns, 210 provided they share the same time axis (first column). In this case, all signals will be processed with the same input parameters, which is convenient for comparison and analysis of dynamic process experiments. The first row may optionally be used to define the axis labels. Three example files with experimental data are available on the Home page. The ILT WebApp can be accessed at <https://nmr-ilt.esalq.usp.br>, and a video tutorial demonstrating its use is available at <https://www.youtube.com/watch?v=jkQeJhQg-Ck>

215 To demonstrate some aspects of the WebApp it will be processed TD-NMR signals from simulated and experimental data. Figure 4a) shows that the input data need to be in *.txt* or *.dat* files, without any text, only the data values in at least two columns, the first one is the time axis and the second the signal amplitude.

220 After the ILT processing, resulting figures are generated in the WebPage. Fig. 4b) shows the relaxation time distribution obtained, with the x-axis in logarithmic scale, d) shows the comparison between the *fitting* and the input signal, and e) its respective residues. All data and figures can be downloaded in a zip file.

## 5 Results and discussions

To evaluate the performance and robustness of the implemented ILT algorithm, a series of tests were conducted using simulated and experimental TD-NMR signals acquired under different conditions for CPMG, Inversion Recovery (IR), and Saturation Recovery (SR) experiments. The results presented below focus on the influence of regularization parameters, the fidelity of the 225 recovered relaxation time distributions, and the consistency of the results with known ground-truth distributions and literature data.

### 5.1 Influence of the regularization parameter $\alpha$

Figure 5 illustrates the effect of the regularization parameter  $\alpha$  on the relaxation time distribution obtained from the ILT of a bi-exponential CPMG signal with relaxation times of 100 ms and 500 ms. As expected, increasing  $\alpha$  leads to broader distributions 230 with reduced peak amplitudes, while preserving the total spectral area. This behavior reflects the trade-off between resolution and stability that is characteristic of regularized inverse problems.

The choice of  $\alpha$  is particularly critical for signals with limited signal-to-noise ratio, where excessive regularization may oversmooth physically relevant features, whereas insufficient regularization can amplify noise-induced artifacts. Although 235 automated optimization strategies such as the L-curve method have been proposed in the literature (Hansen, 1992; Day, 2011), the present implementation allows manual selection of  $\alpha$ , enabling the incorporation of prior knowledge about the sample and experimental conditions.

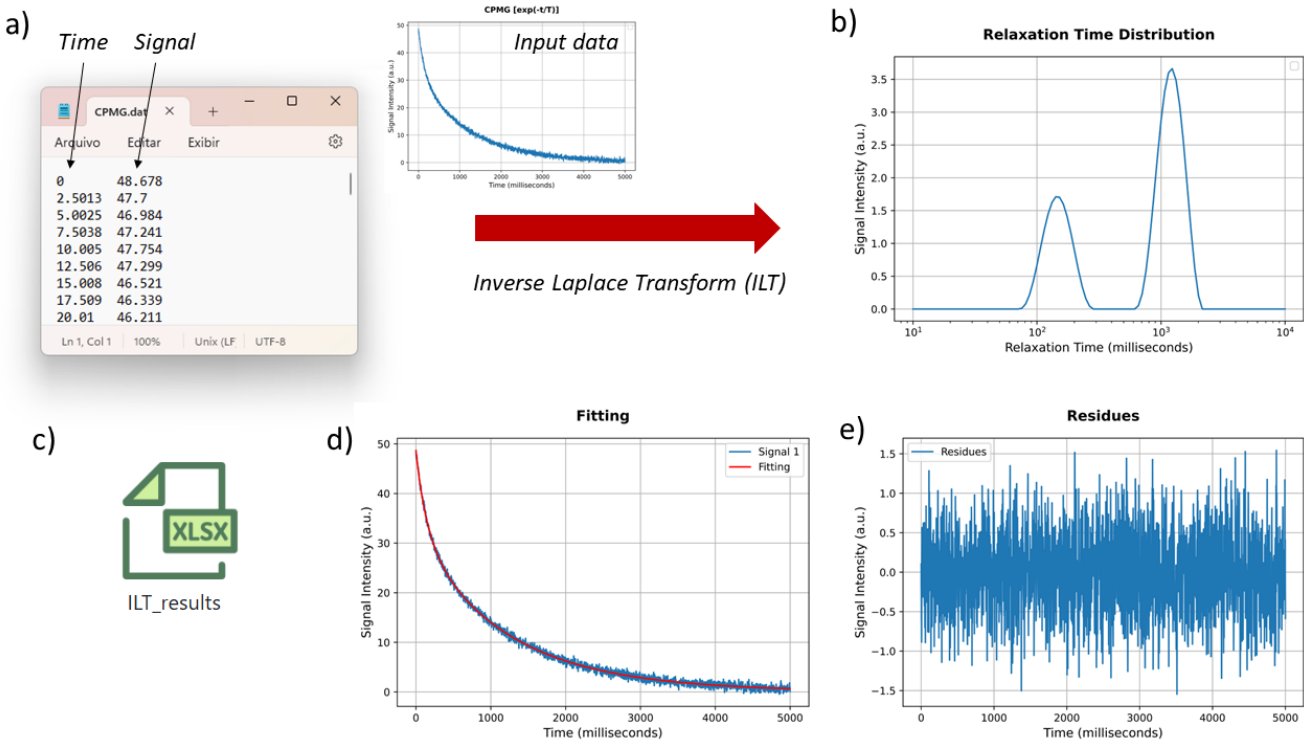


**Figure 4.** The signal input need to have a minimum of two columns: first the time axis and the second with the amplitude signal  $c(t)$ . The results of ILT processing are presented in figures b) to e) with the b) relaxation time distribution, d) comparison of *fitting* and input signal and e) its residues. All data results can be downloaded in a xlsx file.

## 5.2 Validation using simulated and experimental signals

The algorithm was first validated using simulated TD-NMR signals generated from predefined relaxation time distributions. Broad log-Gaussian distributions were used to emulate realistic heterogeneous systems, and synthetic CPMG and IR signals 240 were obtained by numerical integration of these distributions, followed by the addition of Gaussian white noise (RMS = 1%). Figure 6 a,b shows representative simulated signals, while Fig. 6 c,d compares the original distributions with those recovered by the ILT algorithm.

For both CPMG and IR kernels, the recovered distributions exhibit excellent agreement with the ground-truth distributions used in the simulations, accurately reproducing peak positions, widths, and relative amplitudes. The relative deviation of peak 245 centers was below a few percent for all tested cases, consistent with results reported for established ILT implementations in the literature.

Beyond simulations, the algorithm was applied to experimental TD-NMR data acquired from maize seed samples at different hydration and germination stages (Fig. 7). The  $^1H$  TD-NMR measurement were performed on a 11.3 MHz spectrometer (0.27 T for  $^1H$  resonance frequency), SLK-200 (SpinLock, Argentina), using a 30-mm probe at 30 °C. It was used the Carr-Purcell-

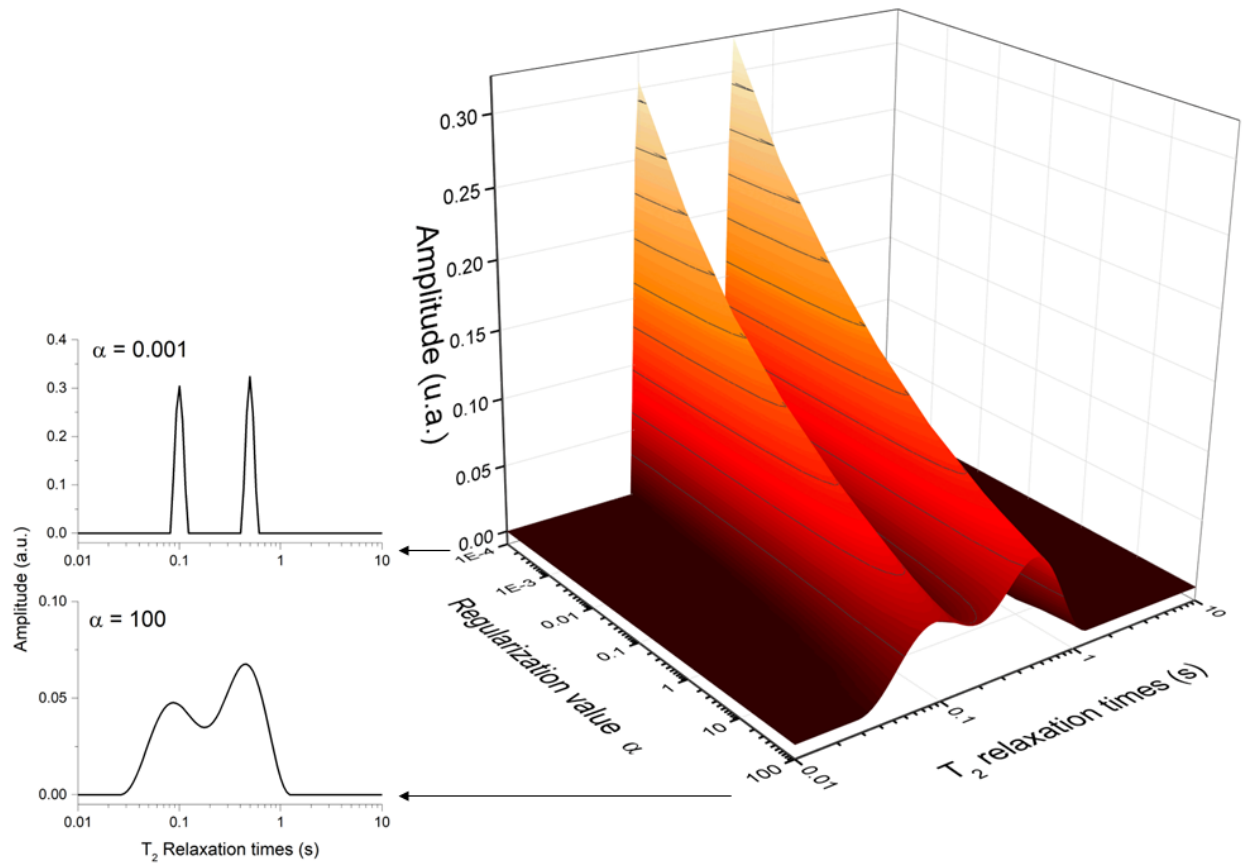


**Figure 5.** Effect of the regularization parameter ( $\alpha$ ) on the resulted relaxation distribution spectrum. The larger the value of  $\alpha$ , the broader the peaks becomes.

250 Meiboom-Gill (CPMG) pulse sequence executed using  $90^\circ$  and  $180^\circ$  pulses of 9.0 and  $18.5\ \mu\text{s}$ , respectively, and echo times of  $200\ \mu\text{s}$ , with a total of 4.000 echoes, a recycle delay of 3 s and 32 scans. For ILT processing, it was used  $\alpha = 1$  and 100 points.

The three ILT spectra of Fig. 7 are from a set of 9 maize seeds measured simultaneously, first in a) measured when they are dry with less than 10% of moisture, in b) measured after the set of maize seeds absorbed water by 24 hours, and in c) after some days when they started germination, as showed in the insert illustration of a maize seed. It can be noted in a) that the 255 main peak at first in  $T_2 = 1\ \text{ms}$ , shifted to  $3\ \text{ms}$  in b), and also get wider. Also, the two smaller peaks in a), around 40 and 150 ms shift and widen in b), these changes reflect the process of water absorption and the increase of heterogeneity inside the maize seeds. These process can be monitored in much more steps, and studied to interpret which each peak represent inside the maize seed. These peaks of  $T_2$  relaxation times in seeds, typically represents signals from different portions of water/oil mobility due the porous structures.

260 In Fig. 7 c) it is presented the ILT spectrum of germinated maize seeds, as showed in the insert illustration of a maize seed. These resulting relaxation time distributions reveal systematic shifts and broadening of the  $T_2$  peaks as water uptake

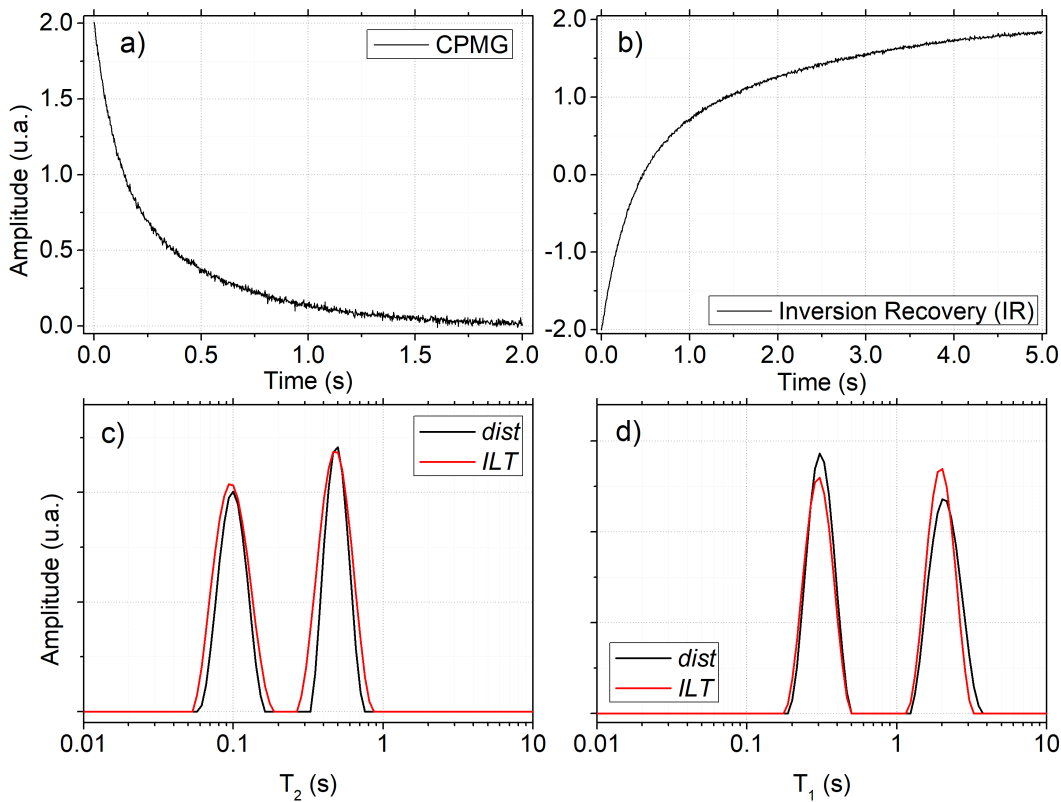


**Figure 6.** Simulated signals of CPMG and IR kernel were created to check the ILT WebApp performance. a) and b) shows the CPMG and IR signals respectively, these signals were created by the integration of an original distribution of relaxation times (*dist*, black line in c) and d)). For CPMG the peaks are centered at 100 ms and 500 ms. For IR the peaks center are 300 and 2000 ms. Therefore, processing the time domain data with ILT, it was obtained the red line (*ILT*) in c) and d) that are the respective spectra of the data above. Several similar simulated data were tested and results are consistent with other ILT softwares.

and metabolic activity increase, reflecting changes in molecular mobility and structural heterogeneity within the seeds. These trends are consistent with previously reported TD-NMR studies of maize seeds and validate the applicability of the proposed approach to real agro-biological systems (Song et al., 2022).

265 Taken together, these results demonstrate that the implemented ILT algorithm reliably recovers relaxation time distributions from both simulated and experimental TD-NMR data, producing results consistent with established methods. Moreover, the same core algorithm has been successfully applied by our research group in a wide range of previous studies, including food analysis (Moraes and Colnago, 2022), meat aging and color evaluation (Cônsolo et al., 2021; Moreira et al., 2016), physiological disorders in poultry and fruits (Cônsolo et al., 2020; Bizzani et al., 2020), seed and plant science (Monareto et al., 2021), enzymatic activity in cassava roots (da Silva Ferreira et al., 2018), and the detection of counterfeit spirits (de Lima et al., 2023), further supporting its robustness and practical applicability.



### 5.3 Tips and tricks

To ensure accurate analysis of the ILT processing, certain practical aspects need to be emphasized, as illustrated in Figure 8:

275 i) Signals with exponential decay/growth should be entirely measured in the experimental stage, with a sufficiently long baseline. Discontinuities in the initial points or a step in the final baseline, similar to the illustration i), can lead to artificial (spurious) peaks in the resulting ILT spectrum;

ii) Artificial peaks may arise in the ILT spectrum from slight displacements of the baseline (amplitude offset). To address this, the WebApp provides the option of a pre-processing function "Force to zero/center" for this correction;

280 iii) The ILT spectrum is strongly influenced by the signal-to-noise ratio of the acquired data. Noisy experimental signals can result in unreliable distributions;

iv) Note that the ILT spectrum will have the same time unit as the input signal. We recommend using times in seconds or milliseconds for the input signal, as relaxation times of biologic samples typically fall within the range of 0.001 s and 10 s.

v) Note that the ILT spectrum window (Starting T value and Ending T value) and the number of points (100) must be selected carefully. If the window is too short or too long, it can generate distributions with artificial and distorted peaks;

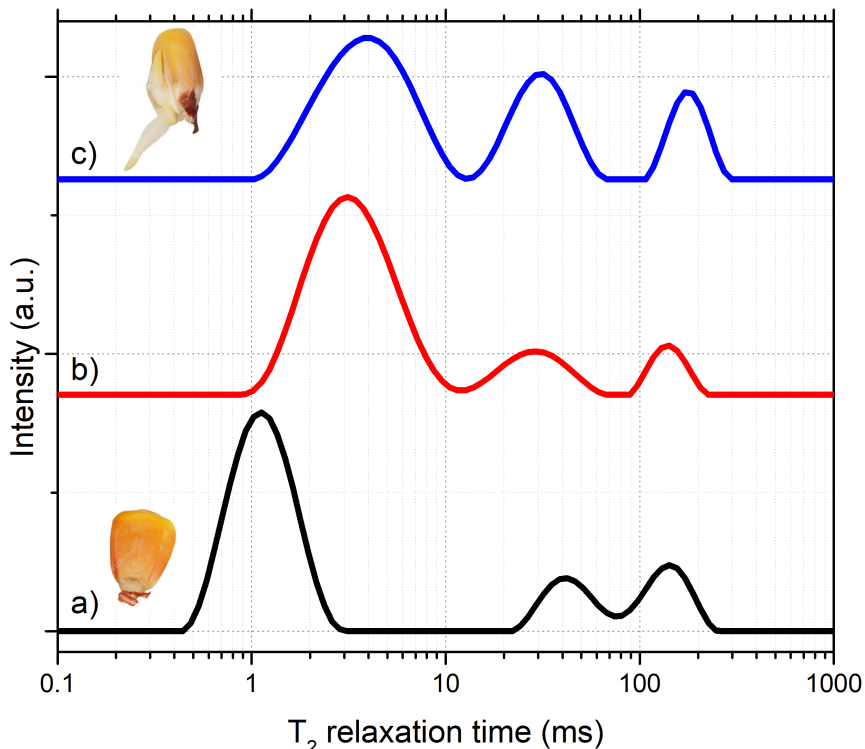


**Figure 7.** Comparison of the relaxation time distribution of maize seeds, in a) dry with less than 10% of moisture, b) after the set of maize seeds absorbed water by 24 hours, and in c) after some days when they started germination, as presented in the upper insert illustration of the maize seed. These results are consistent with Song et al. analysis of maize seeds (Song et al., 2022).



285 vi) For studies comparing several signals, it is advisable to consistently use the same parameters values in both the experimental acquisition stage and in the ILT processing. For the ILT processing these parameters include the number of points,  $\alpha$  parameter, and the values of Starting T value and Ending T value.

By paying attention to these practical considerations, more accurate and meaningful ILT analyses can be achieved.

## 6 Conclusion

290 This work presented the fundamental principles of the Inverse Laplace Transform (ILT) applied to time-domain NMR (TD-NMR) data and introduced an open-access WebApp designed to perform this analysis in a transparent and platform-independent manner. The implemented approach is based on non-negative least squares combined with Tikhonov regularization, providing a robust framework for the inversion of ill-posed relaxometry problems commonly encountered in TD-NMR experiments.

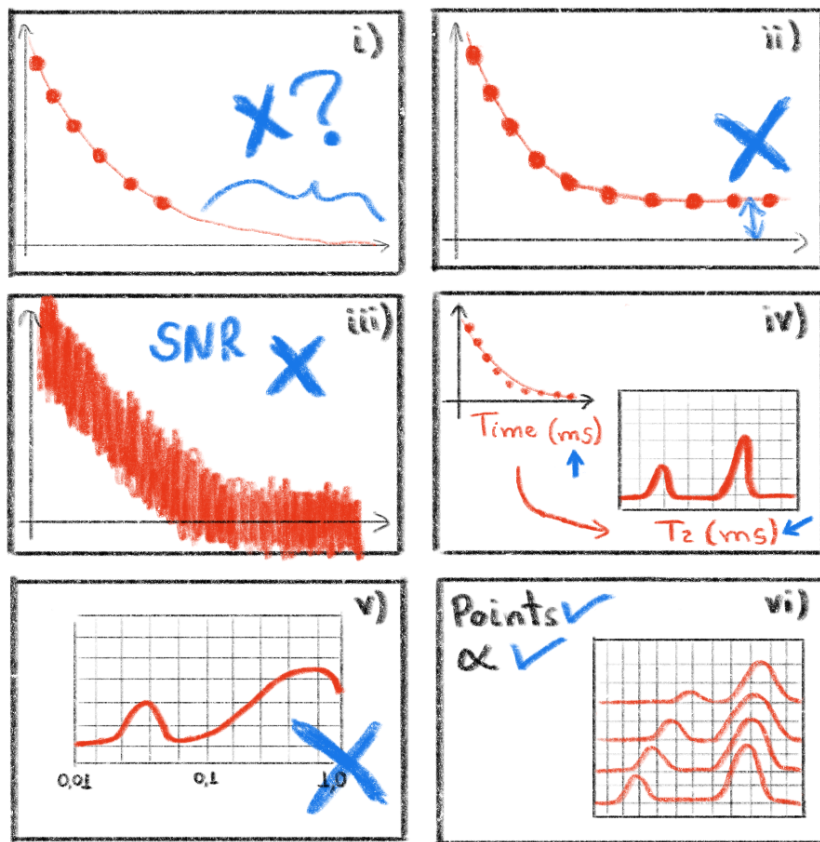


**Figure 8.** Illustration with tips and tricks that must be observed when processing signals with the ILT WebApp. i) shows the problem of discontinuity experimental data signal, ii) offset amplitude, iii) signal-to-noise ratio, iv) time axis, v) selection of an expected window of relaxation times and vi) uses of same parameters values to compare several signals.



Validation using both simulated datasets with known ground-truth distributions and representative experimental signals  
295 demonstrated that the proposed implementation reliably recovers relaxation time distributions, yielding results consistent with those obtained using established ILT software. These findings confirm the methodological soundness of the algorithm and support its use as a complementary tool for TD-NMR data analysis in research and educational contexts.

The WebApp is freely accessible online at <https://nmr-ilt.esalq.usp.br/>, offering an accessible environment for ILT analysis without the need for proprietary software. Future developments will focus on extending the available functionalities and  
300 incorporating automated strategies for regularization parameter selection.

## Acknowledgments

The authors would like to thank the University of São Paulo (USP) and Instituto Federal de Educação, Ciência e Tecnologia de São Paulo (IFSP), campus de Piracicaba/SP for supporting the development of this project. This work was financially supported by the following Brazilian agency Conselho Nacional de Desenvolvimento Científico e Tecnológico CNPq grant  
305 (306611/2022-8) and Fundação de Amparo à Pesquisa do Estado de São Paulo FAPESP (2025/09284-9).

*Code availability.* Code is not publicly available.

*Data availability.* Data are available from the authors upon request.

*Code and data availability.* Code is not publicly available. Data are available from the authors upon request.

*Sample availability.* Samples are available from the authors upon request.

310 *Video supplement.* <https://www.youtube.com/watch?v=jkQeJhQg-Ck>

*Author contributions.* T.B. Moraes: Conceptualization, Methodology, Validation, Data curation, Writing – review editing, Funding acquisition, Supervision, Project administration; G.V. Von Atzingen: Software, Data processing, Formal analysis, Writing – original draft; L.P. Mazzero: Software, Web platform development, Implementation; W.S. Mendes: Software, Web platform development, Implementation; M.B. Zacharias: Investigation, Experimental data acquisition, Validation, Writing – original draft; M.C.B. Cardinali: Software, Data processing,  
315 Methodology, Writing – review editing.



*Competing interests.* The authors declare that they have no competing interests.

*Acknowledgements.* The authors would like to thank the Universidade de São Paulo (USP) and Instituto Federal de Educação, Ciência e Tecnologia de São Paulo (IFSP), campus de Piracicaba/SP for supporting the development of this project. This work was financially supported by the following Brazilian agency Conselho Nacional de Desenvolvimento Científico e Tecnológico CNPq grant (306611/2022-8)

320 and Fundação de Amparo à Pesquisa do Estado de São Paulo FAPESP (2025/09284-9).



## References

Arfken, G. B. and Weber, H. J.: Mathematical Methods for Physicists, Academic Press: San Diego, 4 ed., 1995.

Berman, P., Levi, O., Parmet, Y., Saunders, M., and Wiesman, Z.: Laplace Inversion of Low-Resolution NMR Relaxometry Data Using Sparse Representation Methods, *Concepts in magnetic resonance. Part A, Bridging education and research*, 42, 72–88, 2013.

325 Bizzani, M., William Menezes Flores, D., Bueno Moraes, T., Alberto Colnago, L., David Ferreira, M., and Helena Fillet Spoto, M.: Non-invasive detection of internal flesh breakdown in intact Palmer mangoes using time-domain nuclear magnetic resonance relaxometry, *Microchemical Journal*, 158, 105 208, [https://doi.org/https://doi.org/10.1016/j.microc.2020.105208](https://doi.org/10.1016/j.microc.2020.105208), 2020.

Blümich, B.: Introduction to compact NMR: A review of methods, *TrAC Trends in Analytical Chemistry*, 83, 2–11, <https://doi.org/https://doi.org/10.1016/j.trac.2015.12.012>, sI: Compact NMR, 2016.

330 Blümich, B., Haber-Pohlmeier, S., and Zia, W.: Compact NMR, De Gruyter, 2014.

Borgia, G., Brown, R., and Fantazzini, P.: Uniform-Penalty Inversion of Multiexponential Decay Data, *Journal of Magnetic Resonance*, 132, 65–77, <https://doi.org/https://doi.org/10.1006/jmre.1998.1387>, 1998.

Bortolotti, V., Brizi, L., Fantazzini, P., Landi, G., and Zama, F.: Open2DTool: A Uniform PENalty Matlab tool for inversion of 2D NMR relaxation data, *SoftwareX*, 10, 100 302, <https://doi.org/https://doi.org/10.1016/j.softx.2019.100302>, 2019.

335 Bruker: <https://www.bruker.com>, 2023.

Butler, J. P., Reeds, J. A., and Dawson, S. V.: Estimating Solutions of First Kind Integral Equations with Nonnegative Constraints and Optimal Smoothing, *SIAM Journal on Numerical Analysis*, 18, 381–397, <http://www.jstor.org/stable/2156861>, 1981.

Cônsolo, N. R., Samuelsson, L. M., Barbosa, L. C., Monaretto, T., Moraes, T. B., Buarque, V. L., Higuera-Padilla, A. R., Colnago, L. A., Silva, S. L., Reis, M. M., Fonseca, A. C., da S. Araújo, C. S., de S. Leite, B. G., Roque, F. A., and Araújo, L. F.: Characterization of 340 chicken muscle disorders through metabolomics, pathway analysis, and water relaxometry: a pilot study, *Poultry Science*, 99, 6247–6257, <https://doi.org/https://doi.org/10.1016/j.psj.2020.06.066>, 2020.

Cônsolo, N. R., Silva, J., Buarque, V. L., Samuelsson, L. M., Miller, P., Maclean, P. H., Moraes, T. B., Barbosa, L. C., Higuera-Padilla, A., Colnago, L. A., Saran Netto, A., Gerrard, D. E., and Silva, S. L.: Using TD-NMR relaxometry and 1D 1H NMR spectroscopy to evaluate aging of Nellore beef, *Meat Science*, 181, 108 606, <https://doi.org/https://doi.org/10.1016/j.meatsci.2021.108606>, 2021.

345 da Silva Ferreira, J., Moraes, T. B., Colnago, L. A., and Pereira, F. M. V.: Enzymatic Activity Prediction Using Time-Domain Nuclear Magnetic Resonance (TD-NMR) and Multivariate Analysis: A Case Study Using Cassava Roots, *Applied Magnetic Resonance*, 49, 653–664, <https://doi.org/https://doi.org/10.1007/s00723-018-0995-0>, 2018.

Day, I. J.: On the inversion of diffusion NMR data: Tikhonov regularization and optimal choice of the regularization parameter, *Journal of Magnetic Resonance*, 211, 178–185, <https://doi.org/https://doi.org/10.1016/j.jmr.2011.05.014>, 2011.

350 de Lima, J. T., Zawadzki, S. F., Soares, F. L. F., Salome, K. S., Barison, A., de Moraes, T. B., and D’Oca, C. D. R. M.: The forensic ability of TD-NMR in detecting counterfeit spirits by analyzing bottle caps, *Microchemical Journal*, 191, 108 896, <https://doi.org/https://doi.org/10.1016/j.microc.2023.108896>, 2023.

Engelsen, S. B. and van den Berg, F. W. J.: Quantitative Analysis of Time Domain NMR Relaxation Data, pp. 1–19, Springer International Publishing, Cham, ISBN 978-3-319-28275-6, [https://doi.org/10.1007/978-3-319-28275-6\\_21-1](https://doi.org/10.1007/978-3-319-28275-6_21-1), 2017.

355 FIT: <https://fitinstrument.com/>, 2023.

Fordham, E., Venkataraman, L., Mitchell, J., and Valori, A.: What are, and what are not, Inverse Laplace Transforms, *The Open-Access Journal for the Basic Principles of Diffusion Theory, Experiment and Application*, 29, 1–8, 2017.



Hansen, P. C.: Analysis of Discrete Ill-Posed Problems by Means of the L-Curve, *SIAM Review*, 34, 561–580, <https://doi.org/10.1137/1034115>, 1992.

360 Harris, C. R., Millman, K. J., Walt, S. J., et al.: Array programming with NumPy, *Nature*, 585, 357–362, <https://doi.org/10.1038/s41586-020-2649-2>, 2020.

Istratov, A. A. and Vyvenko, O. F.: Exponential analysis in physical phenomena, *Review of Scientific Instruments*, 70, 1233–1257, <https://doi.org/10.1063/1.1149581>, 1999.

Jacobsen, N. E.: *NMR Spectroscopy Explained*, New Jersey: John Wiley & Sons, Ltd, 2007.

365 Lawson, C. L. and Hanson, R. J.: Solving least squares problems, in: *Classics in applied mathematics*, Cap. 26, 1976.

Magritek: <https://magritek.com>, 2023.

Maus, A., Hertlein, C., and Saalwächter, K.: A Robust Proton NMR Method to Investigate Hard/Soft Ratios, Crystallinity, and Component Mobility in Polymers, *Macromolecular Chemistry and Physics*, 207, 1150–1158, <https://doi.org/https://doi.org/10.1002/macp.200600169>, 2006.

370 Mitchell, J., Gladden, L., Chandrasekera, T., and Fordham, E.: Low-field permanent magnets for industrial process and quality control, *Progress in Nuclear Magnetic Resonance Spectroscopy*, 76, 1–60, <https://doi.org/https://doi.org/10.1016/j.pnmrs.2013.09.001>, 2014.

Monaretto, T., Moraes, T. B., and Colnago, L. A.: Recent 1D and 2D TD-NMR Pulse Sequences for Plant Science, *Plants*, 10, <https://doi.org/10.3390/plants10050833>, 2021.

Moraes, T. B.: Transformada Inversa de Laplace para analise de sinais de Ressonancia Magnetica Nuclear de Baixo Campo, *Química Nova*, 375 44, 1020–1027, <https://doi.org/0100-4042.20170751>, 2021.

Moraes, T. B. and Colnago, L. A.: Noninvasive analyses of food products using low-field time-domain NMR: a review of relaxometry methods, *Brazilian Journal of Physics*, <https://doi.org/10.1007/s13538-022-01055-1>, 2022.

Moreira, L. F. P. P., Ferrari, A. C., Moraes, T. B., Reis, R. A., Colnago, L. A., and Pereira, F. M. V.: Prediction of beef color using time-domain nuclear magnetic resonance (TD-NMR) relaxometry data and multivariate analyses, *Magnetic Resonance in Chemistry*, 54, 800–804, 380 <https://doi.org/https://doi.org/10.1002/mrc.4456>, 2016.

Nanalysis: <https://www.nanalysis.com/>, 2023.

Niumag: <https://www.nmranalyzer.com/>, 2023.

Oxford: <https://nmr.oxinst.com/>, 2023.

Provencher, S. W.: CONTIN: A general purpose constrained regularization program for inverting noisy linear algebraic and integral equations, *Computer Physics Communications*, 27, 229–242, [https://doi.org/https://doi.org/10.1016/0010-4655\(82\)90174-6](https://doi.org/https://doi.org/10.1016/0010-4655(82)90174-6), 1982.

Song, P., Yue, X., Gu, Y., and Yang, T.: Assessment of maize seed vigor under saline-alkali and drought stress based on low field nuclear magnetic resonance, *Biosystems Engineering*, 220, 135–145, <https://doi.org/https://doi.org/10.1016/j.biosystemseng.2022.05.018>, 2022.

SpinLock: <https://www.spinlock.com.ar/>, 2023.

Tikhonov, A. N.: On the solution of ill-posed problems and the method of regularization, *Dokl. Akad. Nauk SSSR*, 151, 501–504, 1963.

390 Van Rossum, G. and Drake Jr, F. L.: Python reference manual, Centrum voor Wiskunde en Informatica Amsterdam, 1995.

Venkataraman, L., Song, Y.-Q., and Hurlimann, M.: Solving Fredholm integrals of the first kind with tensor product structure in 2 and 2.5 dimensions, *IEEE Transactions on Signal Processing*, 50, 1017–1026, <https://doi.org/10.1109/78.995059>, 2002.

Williams, P.: *200 and More NMR Experiments: A Practical Course*, 3rd Edition Edited by S. Berger and S. Braun (University of Leipzig). Wiley-VCH, Weinheim, Germany. 2004. xv + 838 pp. 17 × 24 cm. \$89.95. ISBN 3-527-31067-3., *Journal of Natural Products*, 68, 632–632, <https://doi.org/10.1021/np058231c>, 2005.



Zalesskiy, S. S., Danieli, E., Blümich, B., and Ananikov, V. P.: Miniaturization of NMR Systems: Desktop Spectrometers, Microcoil Spectroscopy, and “NMR on a Chip” for Chemistry, Biochemistry, and Industry, Chemical Reviews, 114, 5641–5694, <https://doi.org/10.1021/cr400063g>, pMID: 24779750, 2014.